

# Forest Fire Clustering: Iterative Label Propagation Clustering and Monte Carlo Validation for Single-cell Sequencing Analysis

Zhanlin Chen<sup>1</sup>, Jeremy Goldwasser<sup>1</sup>, Philip Tuckman<sup>2</sup>, Jason Liu<sup>4</sup>, Jing Zhang<sup>3</sup>, Mark Gerstein<sup>1,4,5,\*</sup>

<sup>1</sup> Department of Statistics and Data Science, Yale University, New Haven, CT 06520, USA

<sup>2</sup> Department of Atmosphere, Oceans, and Climate, Massachusetts Institute of Technology, Boston, MA 02139, USA

<sup>3</sup> Department of Computer Science, University of California, Irvine, CA 92617, USA

<sup>4</sup> Department of Molecular Biophysics and Biochemistry, Yale University, New Haven, CT 06520, USA

<sup>5</sup> Department of Computer Science, Yale University, New Haven, CT 06520, USA

\* pi@gersteinlab.org

## Abstract

With the rise of single-cell sequencing technologies, there is a growing need for robust clustering algorithms to extract deeper insights from data. Here, we introduce an intuitive and efficient clustering method, Forest Fire Clustering, for discovering and validating cell types in single-cell sequencing analysis. Compared to existing methods, our clustering algorithm makes minimum prior assumptions about the data distribution and can provide a point-wise significance value via Monte Carlo simulations for internal validation. Additionally, point-wise label entropies can highlight novel transition cell types *de novo* along developmental pseudo-time manifolds. Lastly, our inductive algorithm has the ability to make robust inferences in an online-learning context. In this paper, we describe the method, provide a summary of its performance against common clustering benchmarks, and demonstrate that Forest Fire Clustering is uniquely suitable for single-cell sequencing analysis.

## Introduction

Clustering analysis is an important task in statistical data analysis and data mining. It has been utilized in a wide variety of application scenarios, from finding interest groups in social networks to detecting fraudulent bank activity [1–5]. In single-cell sequencing analysis, individual cells are clustered and categorized into cell types based on genomic features, especially in detecting subtypes of cancer cells for targeted therapy [6]. However, the presence of rare and unknown cell types could go against previous assumptions about cellular composition [7]. Any prior assumption about the data could bias the analysis and would fail to capture the nuances of rare and potentially influential cell types. In addition, doublet or multiplet cell effect occurs when two or more cells are mistakenly sequenced and tagged as one cell [8–10]. These experimental artifacts show cell type characteristics from two or more cell types and could not be filtered by merely examining the number of sequencing reads per cell. There is currently no effective

method for distinguishing and handling these artifacts, and they severely confound the downstream analysis. Clustering methods for single-cell sequencing analysis should intelligently handle rare cell type discovery, validation, and doublet cell artifact removal.

## Overview of Previous Methods

There are currently many clustering methods, and they can be classified into five general categories: centroid-based, connectivity-based, distribution-based, density-based, and spectral-based methods [11], each briefly described below. Some clustering methods are considered as a hybrid between multiple categories, and each method has their pros and cons for single-cell sequencing analysis.

Centroid-based clustering methods, such as K-means Clustering, rely on optimizing a central vector to find data clusters [12]. Commonly used in single-cell analysis, they heavily parameterize on the number of clusters in the data, and such assumptions could exclude the discovery of rare cell types. These methods also assume a spherical data distribution centered around the central vector and clusters data into a Voronoi diagram, which has diminishing performance in high-dimensional single-cell data. In distribution-based clustering methods, clusters are defined as samples from certain distributions (e.g. gaussian distributions in Gaussian Mixture Models). However, similar to K-means, they are also heavily hyperparameterized by the number and shape of the distributions. In practice, single-cell sequencing data rarely come from simple distributions. Therefore, distribution-based methods do not outline cell clusters along the manifold space.

Connectivity-based clustering methods, also known as Agglomerative or Hierarchical Clustering, iteratively merge data points into the same group based on linkage to obtain a hierarchical structure [13]. These methods make little assumptions about the prior distribution of the data, but the continuous nature of potentially unbalanced dendrograms provides no definitive cut-off between clusters, therefore it cannot definitively detect cell type boundaries for cell group discovery. Density-based clustering methods, such as DBSCAN and OPTICS, produce clusters based on reachability [14, 15]. However, these methods perform poorly on overlapping dense clusters and high-dimensional data due to the pre-defined range parameter, and they occasionally output incomplete clustering results [16].

Spectral-based methods construct data graphs and utilize graph theory concepts. A commonly used single-cell clustering method, Louvain, maximizes modularity to find sub-communities in the graph [17, 18]. These methods can discover the number of communities or clusters in the data indirectly specified the resolution parameter, which is a weaker assumption compared to the K in K-means. However, spectral-based methods cannot validate their clustering results and provide a point-wise significance value for the labels. Further, constructing a KNN graph is computationally slow for large datasets.

## Clustering for Single-cell Sequencing Analysis

Each clustering method makes certain assumptions about the distribution of the data, as reflected by their hyper-parameters. The number and strength of the hyper-parameters influences the clustering results. A suitable clustering method for single-cell analysis should have a small number of parameters for ease of use and make relatively weak assumptions about data distribution. Further, the most challenging aspect of scRNA-seq analysis is how to validate a computational analysis method [33]. To generate clusters with a noisy dataset, it is important to investigate the robustness of the clustering results through internal validation. Previously, Hierarchical Clustering can provide significance values with respect to the label for a group of points using

bootstrap resampling techniques [19]. In contrast, a much more interpretable and useful statistic for single-cell analysis is to calculate a significance value associated with the label at each point, corresponding to the statistical significance of the cell type for each cell. Currently, no method can both cluster the data with little prior assumptions and provide a non-parametric point-wise statistical significance value.

To tackle this challenge, we introduce Forest Fire Clustering, inspired by forest fire dynamics. By modeling label propagation similar to the spread of forest fires, we can cluster data given only a "fire temperature" parameter, similar to the resolution parameter in Louvain. Because Forest Fire Clustering is an iterative process, we can also calculate a permutation-based point-wise significance value by repeated label propagations using Monte Carlo simulations. Lastly, online learning can be a useful feature for analyzing data generated by high-throughput technologies. For example, single-cell sequencing datasets can contain more than a million cells, and clustering once on such a large dataset could take days [20]. As experimental data accumulates over time or as data streams over the network, computational cost of re-clustering continues to rise as the number of cells sequenced increases. Due to the inductive nature of the algorithm, Forest Fire Clustering can be used for online learning and do not need to re-cluster with the arrival of new data.

Here, we provide an overview of Forest Fire Clustering and how it performs against common clustering benchmarks. Additionally, we demonstrate its utility in single-cell sequencing analysis for validating rare cell types, mitigating the doublet cell effect, highlighting novel transition cell types in developmental pseudo-time, and making robust online inferences.

## Results

Clustering complex, high-dimensional single-cell sequencing data efficiently and intuitively is a difficult task. Such a clustering method needs to discover the intrinsic clusters along potentially nonlinear data manifolds, remain robust to noisy outliers in the data, and have a small number of parameters for ease of use. Most importantly, it should detect clustering limitations due to high-dimensionality, and provide a point-wise significance value of the cluster labels for internal validation.

Forest Fire Clustering is designed to meet these specifications. The main idea is to envision data points as trees in a forest, and cluster labels are like multiple fires that propagate through the forest at different times. Modeling forest fire dynamics generates intuitive clusters by iteratively propagating labels through the data manifold. Noisy outliers are de-emphasized as the cluster expands, and there is only one effective parameter that indirectly governs the number of clusters discovered. Additionally, label propagations can be repeatedly simulated to construct point-wise posterior label distributions, which can be used to calculate a permutation-based significance value for internal validation.

There are three main steps in the Forest Fire Clustering algorithm (Fig 1a, b).

1. Preprocessing: Constructing a data graph with data points as vertices and similarities as edges to encode the data geometry. For single-cell analysis, the data matrix  $\mathbf{W}$  with rows as cells and columns as genomic features are used to calculate the cell-to-cell  $L^2$  distance matrix  $\mathbf{M}$ . Then, the distance matrix  $\mathbf{M}$  is transformed into affinities  $\mathbf{A}$  using the kernel method (Step 1-2). The affinity matrix serves as the adjacency matrix of the data graph in a low-dimensional manifold. An adaptive kernel can be used to accurately capture the local structure and the long range interactions between data points.

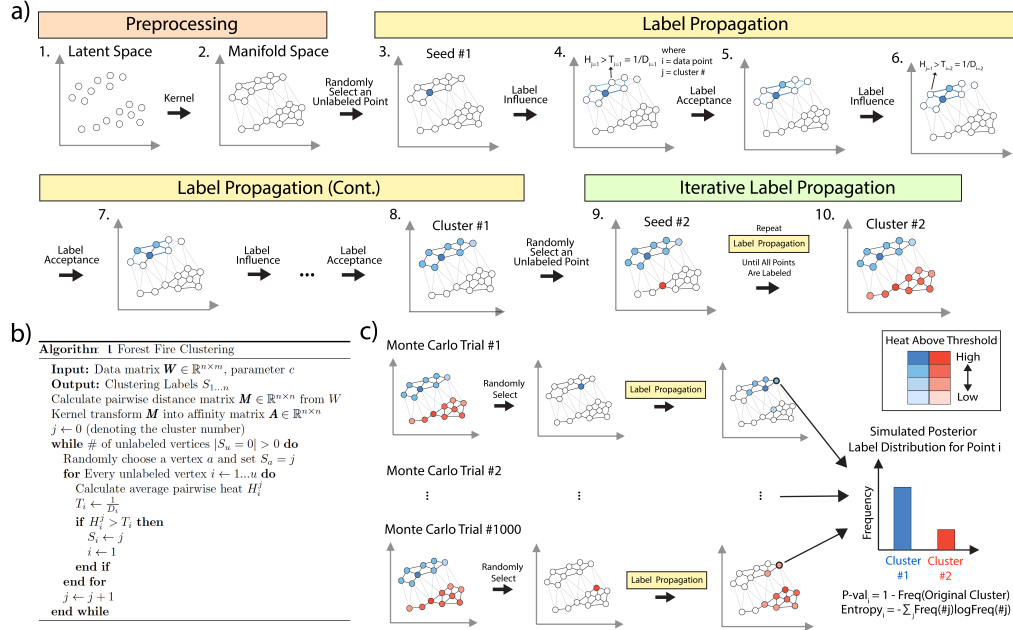


**Fig 1. Illustration of Forest Fire Clustering and Comparison Against Other Clustering Methods:** a) Illustration of Forest Fire Clustering. In the data preprocessing stage, a data graph is created by transforming the pairwise distance into affinities using the kernel method (Step 1-2). Then, a vertex is randomly selected as the seed to take on a label (Step 3). The label is allowed to propagate to other vertices by seeing if the average label influence crosses the threshold at each vertex (Step 3-8). Lastly, the process is iteratively repeated until all vertices have been given a label (Step 9-10). b) Pseudo-code for the Forest Fire Clustering algorithm. c) Monte Carlo simulation procedure to construct an empirical posterior label distribution. The labels from the original round of Forest Fire Clustering are tested for their statistical significance. A seed vertex is randomly chosen while all other labels are cleared. With the same set of parameters, the seed label is allowed to propagate to other vertices until the influence cannot cross thresholds at any other vertices. The process is repeated for many Monte Carlo trials. For each point, the labels over all trials are collected to construct a posterior label distribution, which can be used to calculate the significance value and the Shannon entropy.

$$\mathbf{M} = \|\mathbf{W}\|_2 \quad (1)$$

$$\mathbf{A} = \text{kernel}(\mathbf{M}) \quad (2)$$

2. Label Propagation: Selecting random unlabeled vertices (or seeds) in the data graph to initiate label propagation. We select a random unlabeled vertex as a seed to take on a new label (Step 3). Each unlabeled vertex  $i$  has a label acceptance threshold  $T_i$ , which is defined as the inverse of the degree. Since vertices in dense regions are more likely to be in the same cluster, the inverse relationship lowers the label acceptance threshold near dense regions so those vertices can accept and propagate the labels more easily. The labeled seed radiates a label influence  $H_{seed,i}$  (or heat) to all other unlabeled vertices  $i$  calculated by the affinity  $A_{seed,i}$  multiplied by a user-provided "fires temperature" parameter  $c$ , so the farther unlabeled vertices are from the seed, the less affinity between the vertices, and the less label influence they experience. If the label influence  $H_{seed,i}$  crosses the acceptance threshold  $T_i$ , then the unlabeled vertex takes on the same label as the



seed (Step 4-5). If the label influence  $H_{seed,i}$  is not enough to cross the threshold  $T_i$ , then it might be possible that the average label influence from more labeled vertices is enough to cross the threshold later on (Step 6-7). Therefore, Forest Fire Clustering iteratively checks all vertices until the average label influence is not enough to cross the thresholds for all remaining unlabeled vertices (Step 8).

$$T_i = \frac{1}{D_i} \quad (3)$$

$$H_{seed,i} = c \cdot \bar{A}_{seed,i} \quad (4)$$

3. Iterative Label Propagation: New label propagations are repeated until all vertices have been given a label (Step 9-10). Each label propagation corresponds to a cluster, and vertices labeled from previous iterations are considered exhausted and can no longer take on new labels. This way, nonlinear clusters in the data manifold can be found by propagating along the data geometry. The sparse region between data points separates the label influences and form natural cluster edges, which can be outlined by iterative label propagation.

Using the label propagation dynamic, we can also simulate point-wise posterior label distributions for internal validation and make robust online inferences.

First, we can test the statistical significance of the Forest Fire Clustering labels using Monte Carlo simulations (Fig 1c). The null hypothesis corresponds to whether a data point belongs to any other cluster. In each Monte Carlo trial, a random seed is selected while all other labels are cleared. The label of the seed vertex is allowed to propagate until it can no longer cross the threshold of the remaining unlabeled vertices. Over a large number of Monte Carlo trials, the new labels at each point are tabulated to construct the simulated posterior label distribution, which can be used to calculate a permutation-based significance value and Shannon entropy for the label given to a data point.

Second, clustering labels can be extended to new data points in an online-learning context (Fig S1a). As new data points arrive, we could iteratively check whether label influences from existing clusters can cross the threshold of the new vertex. If multiple clusters can cross the threshold, then the data point takes on the label with the largest influence. If none of the clusters can cross the threshold, then the data point is considered to be in its own cluster with a new cluster label. In contrast with previous online clustering methods, we can discover new clusters in the newly arrived data, which reduces the computational cost for re-clustering and scales in accordance with the growth of high-throughput technologies.

In the sections below, we evaluate Forest Fire for clustering, internal validation, and online learning. However, it is difficult to evaluate the performance of unsupervised tasks without a gold standard. Therefore, two general strategies are used. First, simulations are used to generate data with ground truth labels. We simulated simple synthetic data and single-cell RNA-seq from known distributions. Clustering labels are compared to ground truths with metrics such as accuracy, Adjusted Rand Index (ARI), and Purity Scores. Second, clustering labels on real data were compared against labels generated by domain experts in previous studies. Through these strategies, we show that Forest Fire Clustering can discover robust cell types and generate new insights from single-cell sequencing data.

## Evaluating Forest Fire Clustering on Simulated Data

### Forest Fire Dynamic Provides Insight on the Clustering Process

We first evaluated the performance of Forest Fire Clustering on simulated gaussian mixtures (Fig 2a; left, middle). Two gaussian mixture models ( $\sigma = 0.15$  and  $\sigma = 0.2$ )

were constructed with 8 distributions located evenly around the unit circle ( $n = 500$ ). Forest Fire Clustering generated cluster labels corresponding to each gaussian in the mixture. Because fire temperature  $c$  indirectly parameterizes the size of the clusters, Forest Fire Clustering can infer the number of clusters in the data by detecting cluster edges using sparse regions in the data manifold space.

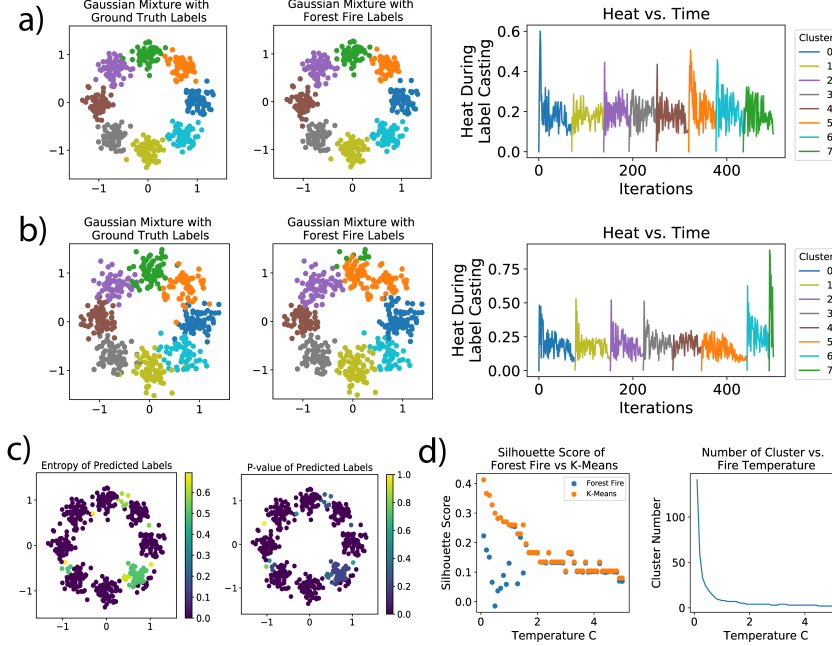


**Fig 2. Gaussian Mixture Models:** (a) Ground truth and Forest Fire Clustering labels on gaussian mixtures ( $\sigma = 0.15$ ) centered around the unit circle, with heat over time plot. (b) Ground truth and Forest Fire Clustering labels on gaussian mixtures ( $\sigma = 0.20$ ) centered around the unit circle, with heat over time plot. (c) Monte Carlo simulations are used to derive the empirical posterior label distribution of each data point on gaussian mixtures ( $\sigma = 0.15$ ) centered around the unit circle. The point-wise entropies are calculated with respect to all of the labels, while the significance values are calculated with respect to the original predicted label. (d) Silhouette score and cluster number of Forest Fire Clustering vs. K-Means Clustering on gaussian mixtures ( $\sigma = 0.15$ ) centered around the unit circle.

Interestingly, the number of clusters can also be inferred from the heat over time plot (Fig 2a; right). The plot records the label influence  $H_i$  of each vertex when it was labeled, which sheds new light on the clustering process and enhances interpretability of the clustering results. As the cluster size increases, the unlabeled vertices becomes farther away from the cluster center. Hence, the label influence for unlabeled vertices decays within each round of label propagation. With a low gaussian bandwidth, every spike corresponds to a meaningful cluster that was discovered. With a higher gaussian variance, eight clusters were discovered, but one cluster has a small number data points (shown in the green cluster). Likewise, the heat over time plot indicated a small spike for that cluster (Fig 2b; right). Therefore, the heat over time plot could be used as a heuristic measure to judge the quality of clustering results.

### Internal Validation Through Monte Carlo Simulation

To internally validate the previous clustering results, posterior label distributions can be constructed by permuting the seed vertex for label propagation via Monte Carlo

simulations, which could be used to calculate a label entropy and significance value for the label of each data point. In Fig 2b and Fig 2c, we show the point-wise label entropies and significance values for the gaussian mixtures. There is more label ambiguity on the edges of certain clusters and over particular clusters. Further, data points on the edges of certain clusters are not statistically significant for the predicted label. In single-cell analysis, the significance value can be used as quality control for robust cell type discovery. All other clustering methods are limited in calculating a similar metric because there is no correspondence between the cluster labels across each iteration.

### **Forest Fire Clustering Generates Near Optimal Clustering Labels**

In addition to internal validation, we also evaluated the quality of the clusters discovered by Forest Fire Clustering. We performed experiments to see if our only effective parameter  $c$  can robust find high quality clusters. We verified our hypothesis that as the fire temperature  $c$  increases, the size of the cluster also increases (Fig 2d; middle). The silhouette score for K-means is locally optimal when given the number of clusters  $K$ . Here, we discovered the number of clusters using Forest Fire Clustering and compared the silhouette score with K-means (Fig 2d; left). As fire temperature  $c$  increases, Forest Fire Clustering converges with K-Means Clustering in silhouette score when given the number of clusters. Because iterative label propagation along the data manifold outlines the edges of clusters, Forest Fire Clustering can also generate approximately optimal clusters. In the Methods section, we also prove that estimated cluster distributions converge to true cluster distributions.

### **Forest Fire Clustering Achieves Robust Online Learning by Discovering Clusters in New Data**

We performed simulated experiments to examine whether Forest Fire Clustering can infer the existence of new clusters in out-of-sample data. With only 4 training clusters ( $\sigma = 0.1$ ), Forest Fire Clustering demonstrated robust performance as the number of unseen clusters in the out-of-sample data increases, with average Adjusted Rand Index (ARI) and Purity Score both greater than 0.90 compared to ground truths throughout (Fig S1b-d). Additionally, the out-of-sample cluster discovery remains robust with increasing gaussian noise. However, Forest Fire Clustering can only guarantee robust online-learning performance when the training data is larger than the testing data, because large training datasets create robust label manifolds which are less impacted by various testing data arrival sequences.

### **Comparison with Existing Clustering Methods on Synthetic Data**

As mentioned previously, Forest Fire Clustering is designed to overcome weaknesses of existing clustering methods on single-cell sequencing datasets (Fig 3a). In particular when compared with other clustering methods, Forest Fire Clustering can generate clusters with minimum prior assumptions about the data and calculate a non-parametric point-wise significance value. In addition to those unique advantages, we benchmarked Forest Fire Clustering with existing clustering methods on a large number of simple synthetic datasets, shown in Fig 3b. Compared to centroid based methods, Forest Fire labels span over the data manifold space rather than the original data space. Further, Forest Fire Clustering can better uncover the number and size of the clusters, in contrast to connectivity-based and distribution-based methods. Forest Fire Clustering also maintains robust performance in scenarios with overlapping clusters, whereas density-based methods like DBSCAN and OPTICS perform poorly on those

cases and output incomplete clustering results (with undefined points in black). Lastly, Forest Fire Clustering has similar accuracy but a significantly faster runtime compared to Louvain because Forest Fire Clustering does not need to construct a KNN graph.

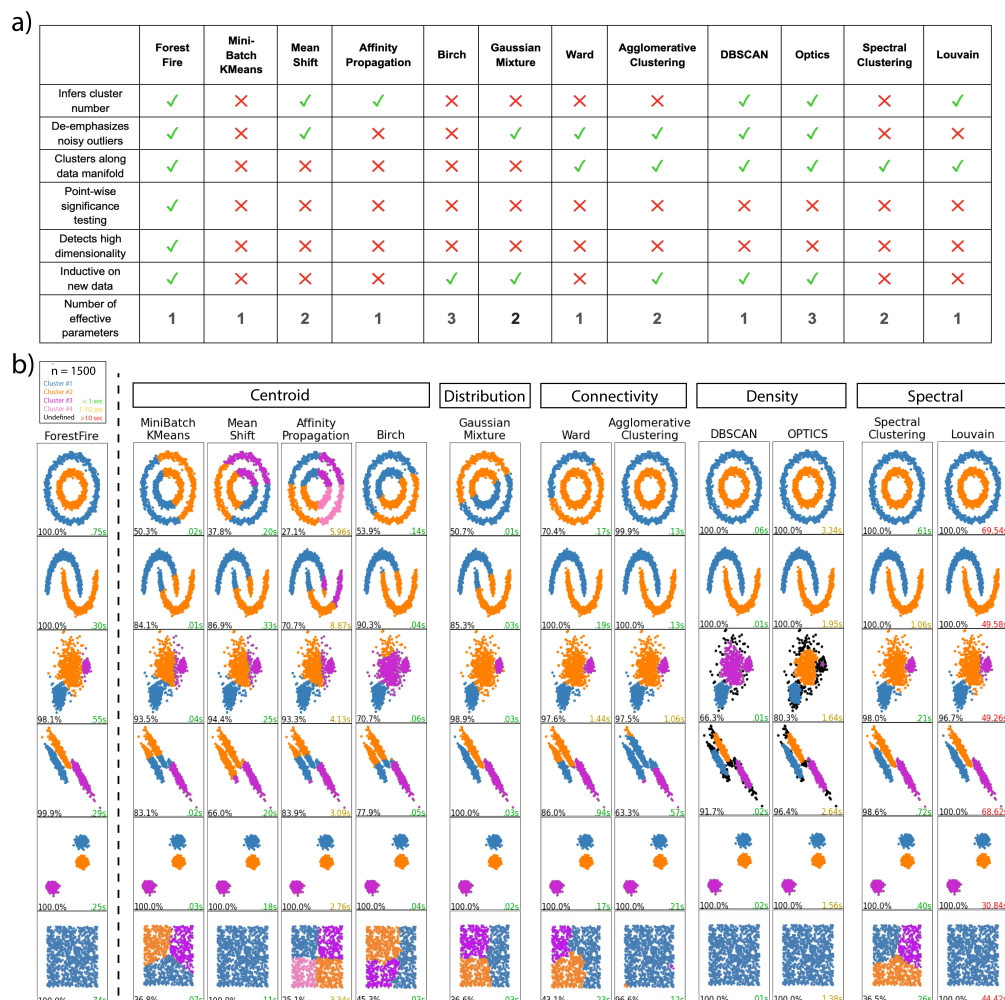


**Fig 3. Comparing Forest Fire Clustering Against Other Clustering Methods on Synthetic Datasets:** a) Table comparing Forest Fire Clustering with existing clustering methods. b) Benchmarking Forest Fire Clustering with other types of clustering methods on common synthetic datasets (with  $n = 1500$ ). Lower left denotes the accuracy, and lower right records the runtime (green  $\leq 1s$ ; yellow  $> 1s$  and  $\leq 10s$ ; red  $> 10s$  ).

## Evaluating Forest Fire Clustering on Simulated Single-cell RNA-seq Data

SC3 and Seurat are considered the most favorable and widely used single-cell clustering methods [21–23]. In particular, SC3 performs hierarchical clustering on a consensus matrix constructed by repeated K-Means Clustering on different partitions of the Laplacian eigenvectors, and Seurat maximizes the modularity in a KNN data graph using Louvain. We compared the performance of Forest Fire Clustering with SC3 and Seurat on simulated scRNA-seq data. Using the Splatter package in R, two types of

simulated data were generated for benchmarking [24]. Group-level simulations generate a mixture of cell populations, and path-level simulations generate stem cells along paths of differentiation. 20 datasets were simulated for each type.

For group-level simulations (Fig 4a), the results show that Forest Fire Clustering outperforms SC3 in ARI and Purity Scores (Signed-rank Wilcoxon  $p = 9.5 \times 10^{-7}$ ). Additionally, Forest Fire Clustering outperforms Seurat in ARI (Signed-rank Wilcoxon test  $p = 7.7 \times 10^{-5}$ ) but has no statistically significant difference in Purity Score, indicating that both Forest Fire Clustering and Seurat can generate homogenous clusters yet Forest Fire Clustering is better at correctly discovering the intrinsic number of cell types and sub-communities. Further, Forest Fire Clustering also outperforms SC3 and Seurat in runtime with an average of 30 seconds compared to 12 minutes and 1 minute, respectively.

The same performance extends to path-level simulations as well (Fig 4b). Moreover, we found that the label entropy of a cell negatively correlates with the pseudo-time steps along the paths of differentiation (Fig 4c, d). As novel transition cells differentiate and become more specialized along the developmental trajectories, the identity of the cells also becomes more deterministic. Point-wise label entropy through Forest Fire internal validation can capture the change in the uncertainty of the cell identity; transition cells tend to have high label entropy, and differentiated cells tend to have low label entropy. Therefore, Forest Fire Clustering can highlight novel transition populations in developmental pseudo-time and lend deeper insights into single-cell analysis compared to existing clustering methods.

## Evaluating Forest Fire Clustering on Real Single-cell RNA-seq Data

To demonstrate the utility of Forest Fire Clustering, we analyzed two types of single-cell transcriptomic experiments. For rare cell type discovery, three single-cell RNA-seq datasets were clustered and internally validated [25–27]. For cell path identification, two stem-cell differentiation single-cell RNA-seq datasets were clustered, and their developmental pseudo-time were analyzed. [28, 29].

For group analysis, high-dimensional genomic features were reduced with t-SNE, and the low-dimensional embeddings were clustered using Forest Fire Clustering (Fig 5a). Our clustering results corroborate with ground truth conclusions from the original studies, with Purity Score  $> 0.7$  and ARI  $> 0.4$  across all three experiments. We also performed internal validation and calculated point-wise significance values. Cells statistically significant for their cluster labels have a higher ARI and Purity Score across all three experiments (Fig 5b). Additionally, we simulated heterotypic doublets using the cells in *Harris et al.* and found that doublet artifacts are less significant for their labels (Fig 5c). Therefore, the point-wise significance value can be used as a metric for validating the discovery of rare cell types and removing doublet cells artifacts.

Further, we evaluated the performance of Forest Fire Clustering in an online learning context. *Macosko et al.* and *Shekhar et al.* are both single-cell RNA-seq on mouse retinal bipolar cells. *Macosko et al.* was clustered first, and the labels were extended to *Shekhar et al.* after removing batch effects. The out-of-sample Purity Score and ARI for *Shekhar et al.* were 0.95 and 0.44, similar to when both experiments were clustered together (Fig S1d). Overall, the out-of-sample performance shows that Forest Fire Clustering can robustly discover new cell types in an online-learning context. The difference in out-of-sample metrics can be attributed to the lack of accurate true cell type labels for benchmarking, especially across single-cell RNA-seq experiments.

For path analysis in both datasets, cells were clustered after preprocessing and dimensionality reduction, and point-wise entropies were calculated via Monte Carlo

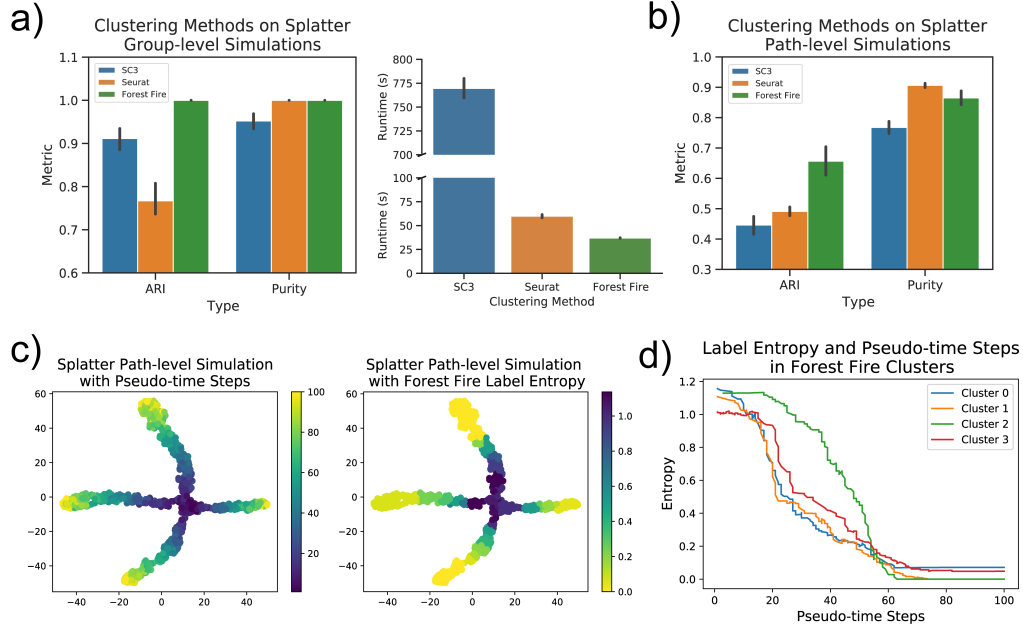


**Fig 4. Simulated Single-Cell RNA-seq Analysis** a) Splatter group-level simulation performance benchmark between SC3, Seurat, and Forest Fire Clustering. With 5 cells groups, Forest Fire Clustering outperforms SC3 and Seurat in ARI and SC3 in Purity Score. Additionally, Forest Fire Clustering outperforms SC3 and Seurat in runtime. b) Splatter path-level simulation performance benchmark between SC3, Seurat, and Forest Fire Clustering. With 4 cell developmental paths, Forest Fire Clustering outperforms SC3 and Seurat in ARI and SC3 in Purity Score. c) In the path-level simulation, a stem cell type differentiates into four cell types. As pseudo-time step increases, the each cell type becomes more specialized. Forest Fire entropy is able to mimic the pseudo-time step along the data manifold. d) Negative correlation between label entropy and pseudo-time step of each cell. As the differentiation pseudo-time step increases, the label entropy decreases, indicating that cell identities becomes more deterministic in the manifold space.

Simulations (Fig 6a). Forest Fire clusters were used to construct PAGA topology maps for visualization [30]. In the data from *Paul et al.*, mouse Hematopoietic Stem Cells (HSCs) were identified using signature gene expression (*Procr*) and were used as roots for diffusion pseudo-time calculations [31]. The stem cells in diffusion pseudo-time analysis coincides with novel transition cells highlighted by Forest Fire label entropy. To identify stem cells and outline their relationship with other cells, diffusion pseudo-time analysis utilizes a top-down approach by assuming prior knowledge of stem cells *a priori* (e.g. signature gene expression). In this case, making wrong assumptions about the signature genes expressed in stem cells could lead to choosing the wrong root for diffusion. However, bottom-up approaches like Forest Fire Clustering do not make those assumptions and can empirically reveal novel transition cells along the data manifold. By initiating label propagation from various cells in their developmental trajectories, Forest Fire Clustering can find novel transition cell types at the intersection of those label propagations where the label entropy is high. Therefore, Forest Fire Clustering can naturally uncover branching points in developmental trajectories. This capability is further demonstrated with single-cell RNA-seq data from *Moon et al.* where human embryonic stem cells (hESC) were sequenced with single-cell RNA-seq along 3, 5, 7, and

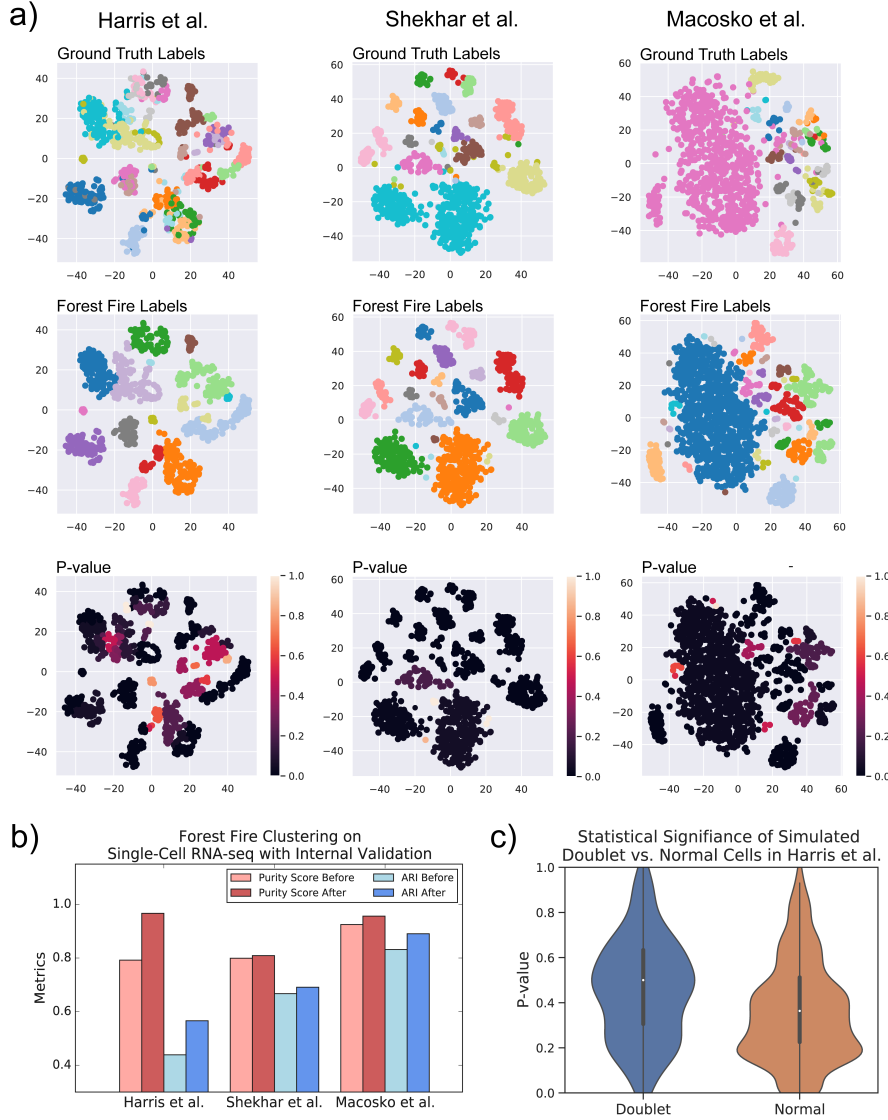


**Fig 5. Cell Group Analysis:** a) Forest Fire Clustering was performed on three single-cell RNA-seq experiments. The resulting labels corroborated with ground truth labels from previous studies. Internal validation was performed to evaluate the significance of rare cell types and to mitigate the doublet cell effect. b) Across all three experiments, cells significant for their cluster labels after internal validation have a higher Purity Score and ARI compared to cells before internal validation, indicating that significance values can be used for quality control and validating cell type definitions. c) Artificial doublets were created by merging cells from different clusters in *Harris et al.*. Internal validation shows that doublet cells are less significant for their given label, indicating that point-wise significance values can be a useful metric for doublet detection and quality control.

9 developmental days (Fig 6b). The analysis shows that Forest Fire label entropies mimic real developmental time and can be used to generate deeper insights for single-cell sequencing analysis.

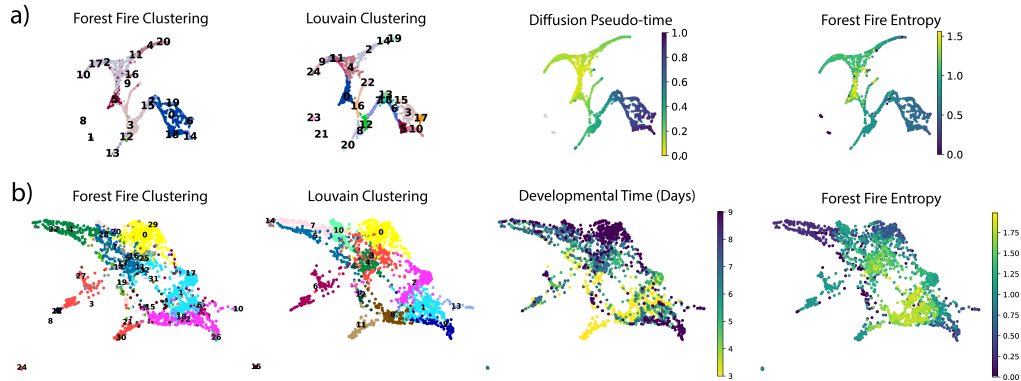


**Fig 6. Cell Path Analysis:** a) For *Paul et al.*, PAGA topology maps were generated using Forest Fire Clustering. Diffusion pseudo-time were calculated by choosing the Louvain clusters with mHSC signature gene expression. The diffusion trajectories are similar to the pattern highlighted by Forest Fire entropy. b) For *Moon et al.*, PAGA topology maps were also generated with Forest Fire Clustering. Developmental trajectories of hESCs were highlighted using Forest Fire entropy without prior knowledge of stem cell types.

## Evaluating Forest Fire Clustering on Other Biological Datasets

To explore the utility of Forest Fire Clustering on other biological datasets, we evaluated the performance of Forest Fire Clustering on malignant tumor classification [32]. The dataset contains 569 tumor samples each with 32 features and labels on whether the sample is malignant or benign (Fig S1). Visualization using the first two principle components of the features shows a separation along tumor malignancy with ambiguity near the overlap. K-Means Clustering and Louvain Community Detection both separated the data near the intersection of labels (ARI of 0.49 and 0.41, Purity Score of 0.85 and 0.82, respectively). Similar to Louvain, Forest Fire Clustering also found two clusters in the data. However, Forest Fire Clustering outperformed K-Means and Louvain with an ARI of 0.65 and Purity Score of 0.91. Furthermore, the internal validation showed high entropy near the intersection of the labels. K-Means and Louvain both separated the data around the high entropy region, but Forest Fire Clustering separated the data along the points with the highest entropies. Because Forest Fire Clustering averages the influence from a cluster, our approach can accurately approximate the center of clusters and precisely outline the edges between clusters.

As the number of dimensions in the dataset increases, the distance between data points becomes more uniform, which decreases the signal-to-noise ratio when distinguishing data points from one another. Similar to all other clustering methods, high dimensional data geometry also negatively impacts the performance of Forest Fire Clustering. However, our approach can detect those limitations through internal validation. Homogenous data points tend to have higher label entropies and larger significance values. In contrast with other clustering methods, Forest Fire Clustering has the unique advantage of directing users away from pitfalls in high dimensional data. In practice, dimensionality reduction techniques such as t-SNE, UMAP, or PCA are recommended as a preprocessing step before clustering high dimensional datasets.

## Discussion

Clustering analysis labels and classifies data by identifying the commonalities in the features. As an unsupervised learning technique, it has been used in a wide variety of



application scenarios. In particular, the recent rise in single-cell sequencing relies on clustering methods to discover rare, novel cell types based on genomic features.

However, there are many open challenges associated with unsupervised clustering of single-cell RNA-seq data [33]. Previous clustering methods parameterizes heavily on prior assumptions about the data and do not provide a way to internally validate the results. For single-cell sequencing analysis and many other scientific applications that deal with noisy data, it is important to both intelligently cluster with minimum prior assumptions and report the statistical significance of the result labels for validation.

To tackle these challenges, we propose Forest Fire Clustering inspired by forest fire dynamics. By reformulating label propagation to iteratively find clusters in the data manifold space, Forest Fire Clustering offers an efficient and intuitive approach to clustering data. With only one effective parameter that indirectly governs the size of the clusters, our method can discover the number of clusters in the data with minimum prior assumptions. Further, Forest Fire Clustering can conduct internal validation using Monte Carlo simulations. Result labels are propagated repeated to produce a non-parametric point-wise significance value, which could be used for quality control. The label entropies can also be calculated to reveal branching points and highlight novel transition cells along developmental pseudo-time.

Our method outperforms previous clustering methods on common benchmarks and has robust performance on single-cell transcriptomic datasets. Guided by clustering and internal validation results, Forest Fire Clustering can be used to discover rare cell types and mitigate experimental artifacts in single-cell RNA sequencing experiments. The future of single-cell sequencing analysis is to construct a cell-to-cell communication network using interactions between different cell types [34]. Our method offers the possibility of generating robust cell type definitions for network construction and analysis. In addition to single-cell sequencing, our method can be generalized to problems in other domains that involve clustering and evaluating the statistical significance of the result labels.

## Materials and methods

### Forest Fire Clustering

Given a set of data points,  $x_1, \dots, x_n$  each with  $m$  features arranged in a data matrix  $\mathbf{W} \in \mathbb{R}^{n \times m}$ , we calculate the distance matrix  $\mathbf{M} \in \mathbb{R}^{n \times n}$  containing the  $L^2$  distance between every pair of data points. Distances are converted into affinities  $\mathbf{A} \in \mathbb{R}^{n \times n}$  using the kernel method [35]. We can use a gaussian kernel or an adaptive kernel based on K-nearest neighbors to preserve local distances and encode longer trajectory structures (S1 Eq). By doing so, a similarity graph  $G = (V, E)$  is constructed, with each vertex  $v_i$  representing a data point  $x_i$  and the corresponding pairwise affinities as edges. The affinity matrix  $\mathbf{A}$  acts as the adjacency matrix for graph  $G$ .

In short, we iteratively cast a label on a vertex and allow the label to propagate until an equilibrium is reached. If one label cannot propagate to all vertices, the procedure is repeated with different labels until all of the vertices in  $G$  have been given a label. Each vertex  $i$  starts without a label, corresponding to the state  $S_i = 0$ , and accepts a label  $S_i = j$  during the  $j$ -th label propagation.

$$S_i = \begin{cases} j, & H_i^j \geq T_i \\ 0, & H_i^j < T_i \end{cases} \quad (5)$$

$T_i$  is the threshold above which a vertex would accept a label from neighboring vertices, and the heat  $H_i^j$  is the influence from neighboring labels on vertex  $i$  during the

$j$ -th label propagation. These values parameterize the label propagation, similar to how they govern forest fire dynamics.

### Threshold for Accepting Neighboring Labels

The label acceptance threshold  $T_i$  is analogous to flashpoints in forest fire dynamics. A tree in a forest would start burning when the heat surrounding it reaches a certain level, which corresponds to  $T_i$  of a vertex  $i$  in graph  $G$ . In order for label propagation to slowly stop at the cluster edges where the data is sparse,  $T_i$  should be closely related to the density of the graph. Therefore,  $T_i$  is defined to be the inverse of the degree of a vertex  $D_i$ . As the degree  $D_i$  increases, the threshold  $T_i$  for accepting a label decreases. Then, label propagation drifts towards regions of high data density to find the cluster centers.

$$T_i = \frac{1}{D_i} \quad (6)$$

### Heat and Fire Temperature

In a forest fire, heat decays non-linearly with increasing distance and is proportional to the fire temperature. Here, the kernel affinity between two vertices  $i_1$  and  $i_2$  is used to model the non-linear decay in heat as distance increases, and the user-determined parameter  $c$  governs the fire temperature. The pairwise heat between two vertices  $i_1$  and  $i_2$  during the  $j$ -th label propagation is defined as follows.

$$H_{i_1, i_2}^j = c \cdot A_{i_1, i_2} \cdot \mathbb{I}(j\text{-th label propagation}) \quad (7)$$

Centered around an unlabeled vertex  $i$ , heat accumulates from vertices with label  $j$  during the  $j$ -th label propagation. Therefore, heat  $H_i^j$  can be modeled as the average pairwise heat between the unlabeled vertex  $i$  and all vertices with label  $j$ .

$$H_i^j = \frac{\sum_{i_2=1}^n \mathbb{I}(S_{i_2} = j) \cdot H_{i, i_2}^j}{\sum_{i_2=1}^n \mathbb{I}(S_{i_2} = j)} \quad (8)$$

There are two ways to reach a threshold  $T_i$ : by setting a higher fire temperature or by using a kernel with a faster decay. Since using a large kernel bandwidth achieves the same purpose as setting a higher  $c$ ,  $c$  is the only effective parameter in our clustering algorithm. On one hand, higher fire temperatures result in larger clusters, since labels are more likely to spread to other vertices. On the other hand, smaller clusters are discovered by decreasing the fire temperature during label propagation.

For each unlabeled vertex  $i$ , the clustering algorithm recursively checks whether the average heat  $H_i^j$  is higher than the threshold  $T_i$  and adds the vertex to the cluster  $j$  if it is. With  $k$  clusters and  $n$  data points, the algorithm has an approximate runtime of  $O(kn^2)$ . The labels propagate until the following condition is met for every unlabeled point  $u$  at the end of the  $j$ -th label propagation.

$$\{\forall u | S_u = 0, H_u^j < T_u\} \quad (9)$$

After the  $j$ -th label propagation reaches a stopping point, another unlabeled vertex will be randomly selected as the starting vertex for the  $j + 1$ -th label propagation. The algorithm continues until all vertices have been labeled, as shown in the pseudo-code of the algorithm below.

---

**Algorithm 1** Forest Fire Clustering

---

**Input:** Data matrix  $\mathbf{W} \in \mathbb{R}^{n \times m}$ , parameter  $c$   
**Output:** Clustering Labels  $S_{1 \dots n}$   
Calculate pairwise distance matrix  $\mathbf{M} \in \mathbb{R}^{n \times n}$  from  $\mathbf{W}$   
Kernel transform  $\mathbf{M}$  into affinity matrix  $\mathbf{A} \in \mathbb{R}^{n \times n}$   
 $j \leftarrow 0$  (denoting the cluster number)  
**while** # of unlabeled vertices  $|S_u = 0| > 0$  **do**  
    Randomly choose a vertex  $a$  and set  $S_a = j$   
    **for** Every unlabeled vertex  $i \leftarrow 1 \dots u$  **do**  
        Calculate average pairwise heat  $H_i^j$   
         $T_i \leftarrow \frac{1}{D_i}$   
        **if**  $H_i^j > T_i$  **then**  
             $S_i \leftarrow j$   
             $i \leftarrow 1$   
        **end if**  
    **end for**  
     $j \leftarrow j + 1$   
**end while**

---

At the end, our clusters have the following definition. If  $j$  is any cluster, then for vertices  $\{\forall i_1 | S_{i_1} = j\}$  and  $\{\forall i_2 | S_{i_2} \neq j\}$ :

$$T_{i_2} > \frac{\sum_{i_1=1}^n \mathbb{I}(S_{i_1} = j) \cdot H_{i_1, i_2}^j}{\sum_{i_1=1}^n \mathbb{I}(S_{i_1} = j)} \quad (10)$$

$$> c \cdot \frac{\sum_{i_1=1}^n \mathbb{I}(S_{i_1} = j) \cdot A_{i_1, i_2}^j}{\sum_{i_1=1}^n \mathbb{I}(S_{i_1} = j)} \quad (11)$$

## Proof of Forest Fire Clustering

In the following section, we show that Forest Fire Clustering can non-parametrically approximate the true cluster distribution up to the second moment.

Give data points  $X_1 < X_2 < \dots < X_n \sim N(\mu, \sigma^2)$ , Forest Fire Clustering chooses a random point  $X_r$  with heat modeled by the kernel  $N(X_r, \sigma_c^2)$ . The kernel bandwidth  $\sigma_c^2$  is associated with the fire temperature  $c$  and is a user-provided hyper-parameter. Without loss of generality, we assume that  $X_r < \mu$ . Then for the same arbitrary amount of probability  $\epsilon$ , the distance  $|X_{r+1} - X_r|$  is less than  $|X_{r-1} - X_r|$  for  $X$ 's less than  $\mu$ .

$$\int_{X_r}^{X_{r+1}} \frac{1}{\sigma\sqrt{2\pi}} \exp\left(-\frac{1}{2} \left(\frac{x-\mu}{\sigma}\right)^2\right) = \int_{X_{r-1}}^{X_r} \frac{1}{\sigma\sqrt{2\pi}} \exp\left(-\frac{1}{2} \left(\frac{x-\mu}{\sigma}\right)^2\right) = \epsilon \quad (12)$$

$$|X_{r+1} - X_r| < |X_r - X_{r-1}| \quad (13)$$

Hence, the heat from  $X_r$  is more likely to be higher at  $X_{r+1}$  than  $X_{r-1}$  under equal probability.

$$N(X_{r+1}; X_r, \sigma_c^2) > N(X_{r-1}; X_r, \sigma_c^2) \quad (14)$$

Also because  $X_{r-1} < X_r < X_{r+1} < \mu$ ,  $X_{r+1}$  is closer to the true cluster center. It is located in a denser region under the true probability distribution and have a lower label acceptance threshold. Therefore,  $X_{r+1}$  is more likely to receive a label from  $X_r$  compared to  $X_{r-1}$ . If  $X_{r+1}$  receives the label from  $X_r$ , the new heat from  $X_r, X_{r+1}$  is modeled by a normal mixture distribution with mean and variance at  $\hat{\mu}$  and  $\hat{\sigma}^2$ .

$$\hat{\mu} = \frac{X_r + X_{r+1}}{2} \quad (15)$$

$$\hat{\sigma}^2 = \frac{\sigma_c^2 + \hat{\mu}^2 - \mu^2}{2} + \frac{\sigma_c^2 + \hat{\mu}^2 - \mu^2}{2} = \sigma_c^2 + \hat{\mu}^2 - \mu^2 \quad (16)$$

If the fire temperature  $c$  is selected such that  $\sigma_c^2 = \sigma^2$  and heat can cross the threshold of all points  $X_1 \dots X_n \sim N(\mu, \sigma^2)$ , then the mean and variance approaches the expected value and variance of the true cluster distribution by the Law of Large Numbers.

$$\hat{\mu} = \frac{X_1 + \dots + X_n}{n} \rightarrow \mu \quad (17)$$

$$\hat{\sigma}^2 = \frac{\sigma_c^2 + \dots + \sigma_c^2}{n} \rightarrow \sigma^2 \quad (18)$$

The same argument can be generalized to the symmetrical case where  $X_r > \mu$ . With convergence by Law of Large Numbers, the argument can also be generalized to cases where the true cluster distribution is not gaussian. Lastly, we only demonstrated convergence in one dimension, but the argument can be extended to other dimensions in the data.

## Monte Carlo Validation

After all of the vertices are labeled, internal validation can be performed by re-propagating the original labels with Monte Carlo. In the beginning of each Monte Carlo trial, a random vertex takes on the previously clustered label while all other vertices have no labels. With the same set of parameters, the label is allowed to propagate from the initial vertex to all other vertices until it reaches a stopping point. Each iteration is a sample from the posterior distribution of the labels, and the process is repeated for many trials. At each data point, empirical distributions are constructed by tabulating the new labels across Monte Carlo trials. With the simulated posterior probability distribution, point-wise significance values with respect to the original label and point-wise entropies across all labels can be calculated.

---

### Algorithm 2 Monte Carlo Verification

---

**Input:** Affinity matrix  $\mathbf{A} \in \mathbb{R}^{n \times n}$ , parameter  $c$ , original label  $S_{1 \dots n}$ , trial number  $T$

**Output:** Significance value  $P_{1 \dots n}$ , entropy  $E_{1 \dots n}$

Let  $S_{x,t}$  be a state matrix for vertex  $x$  at trial  $t$

**for**  $t \leftarrow 0 \dots T$  **do**

    Randomly choose a vertex  $a$  with original label  $S_a$

**for** Every unlabeled vertex  $i \leftarrow 1 \dots u$  **do**

        Calculate average pairwise heat  $H_i^j$

$T_i \leftarrow \frac{1}{D_i}$

**if**  $H_i^j > T_i$  **then**

$S_{i,t} \leftarrow S_a$

$i \leftarrow 1$

**end if**

**end for**

**end for**

$P_i \leftarrow 1 - \frac{1}{T} \sum_{t=1}^T \mathbb{I}(S_i = S_{i,t})$

$E_i \leftarrow - \sum P_i \log(P_i)$

---

## Analysis of Simulated Data

Gaussian mixtures were generated by sampling from gaussian distributions centered evenly around the unit circle. Two gaussian bandwidths were used in the analysis,  $\sigma = 0.15$  and  $\sigma = 0.2$ . Both sets of gaussian mixture data were clustered with kernel bandwidth  $\sigma = 5$  and fire temperature  $c = 1$ . Simulated data of different shapes were produced by the Sklearn package in Python [36]. For online learning, a dataset with four clusters was simulated and clustered with kernel bandwidth  $\sigma = 5$  and fire temperature  $c = 1$ . Then, another dataset with eight clusters (four of which are from the same distribution as the previous dataset) was simulated and clustered on based on previous labels using the same set of parameters. The performance was evaluated on the out-of-sample data points.

Simulated single-cell RNA-seq were generated using R package Splatter. 1k cells and 5k genes were simulated in one set for 20 datasets. For group-level simulations, five groups were generated (0.45, 0.15, 0.15, 0.15, 0.1) with parameters (*out.prob* = 0.20, *out.facScale* = 1.5), and the cells were clustered with fire temperature  $c = 2500$  and adaptive kernels  $\sigma = 3$ . For path-level simulations, four groups were generated (0.35, 0.25, 0.25, 0.15) with parameters (*out.prob* = 0.1, *out.facScale* = 0.25, *de.prob* = 0.5, *de.facLoc* = 0.2) along differentiation path (0, 0, 0, 0), and the cells were clustered with fire temperature  $c = 850$  and adaptive kernels  $\sigma = 7$ .

There are three main ways to evaluate the performance of unsupervised methods. First, Purity Scores evaluate the cluster labels based on a set of references labels. To calculate the Purity Score, one can construct a confusion matrix and assign the dominant predicted cluster to each ground truth cluster. Then, the sum of the total data points in dominant predicted clusters divided by the total number of data points is the Purity Score. The metric quantifies whether the predicted clusters contain only points from a reference cluster by a value from zero to one. Second, the Adjusted Rand Index (ARI) also measures the similarity between two clusterings. The rand index quantifies whether all pairs of points in two clusterings match up to the same cluster. The ARI is the rand index adjusted for chance. Silhouette scores are also used for performance benchmarking, where it evaluates how similar data points are within a cluster compared to other clusters. However, different from Purity Score and ARI, silhouette score is compared against itself and does not require ground truths to compute the statistic.

## Analysis of Real Data

For cell group analysis, single-cell RNA-seq experiments were acquired from GEO (Accession Number: GSE99888, GSE81904, GSE63472). The expression matrices were normalized with respect to the library size, and the read counts were log-transformed. Each gene was centered and normalized across all cells. Top 10k expressed genes in each experiment were selected, and FIt-SNE was used for dimensionality reduction with PCA initialization and a perplexity of 30 [37]. Forest Fire Clustering was performed using gaussian kernels (with  $\sigma = 6$  and  $c = 300$ ), and the clustering labels were internally validated using the same parameters. Heterotypic doublets were simulated by randomly sampling without replacement pairs of cells from different clusters in *Harris et al.* and adding together the transcript counts between the pair of cells. The original cells used to simulate the doublets were subsequently removed from the count matrix. For online learning, top 10k genes from both experiments were overlapped to obtain a set of 6837 top expressed shared genes. The top genes from both experiments were jointly embedded using FIt-SNE. Forest Fire Clustering was performed on *Macosko et al.* samples using a gaussian kernel (with  $\sigma = 5$  and  $c = 2$ ). Then, the clustering was extended to *Shekhar et al.* using the same parameters. The predicted labels were compared with labels from the respective studies using Purity Score and ARI.

For cell path analysis, *Paul et al.* was downloaded using the Scanpy package [38], and *Moon et al.* was downloaded Mendeley (<https://data.mendeley.com/datasets/v6n743h5ng/1>). Both datasets were preprocessed using the "zheng17" recipe and were clustered with Forest Fire Clustering (with  $\sigma = 6$  and  $c = 850$ ) and Louvain (with  $k = 4, n = 20, resolution = 1$ ). In *Paul et al.*, Louvain cluster 0 and 16 were identified as stem cells by *Procr* mark expression for diffusion pseudo-time analysis. Forest Fire Monte Carlo was performed for 300 rounds in both datasets. The Forest Fire Clusters were used to construct PAGA topology maps for visualization.

Breast cancer malignancy data was downloaded from the UCI machine learning repository [32]. Data features were visualized with PCA, and data points were labeled by the malignancy. Further, the features were clustered using three different methods: K-Means ( $K = 2$ ), Louvain, and Forest Fire. For Louvain, an affinity matrix was constructed using gaussian kernels with  $\sigma = 5$ , and the data was clustered with a resolution of 20. These parameters resulted in 2 clusters in the data. Similarly, Forest Fire Clustering used the same affinity matrix and found 2 clusters with fire temperature  $c = 43$ . Purity score and ARI between the ground truth malignancy and the clustering labels were calculated.

## Supplemental Information

S1 Eq.

$$K_{k,\alpha}(\mathbf{x}, \mathbf{y}) = \frac{1}{2} \exp\left(-\left(\frac{\|\mathbf{x} - \mathbf{y}\|_2}{\varepsilon_k(\mathbf{x})}\right)^\alpha\right) + \frac{1}{2} \exp\left(-\left(\frac{\|\mathbf{x} - \mathbf{y}\|_2}{\varepsilon_k(\mathbf{y})}\right)^\alpha\right) \quad (19)$$

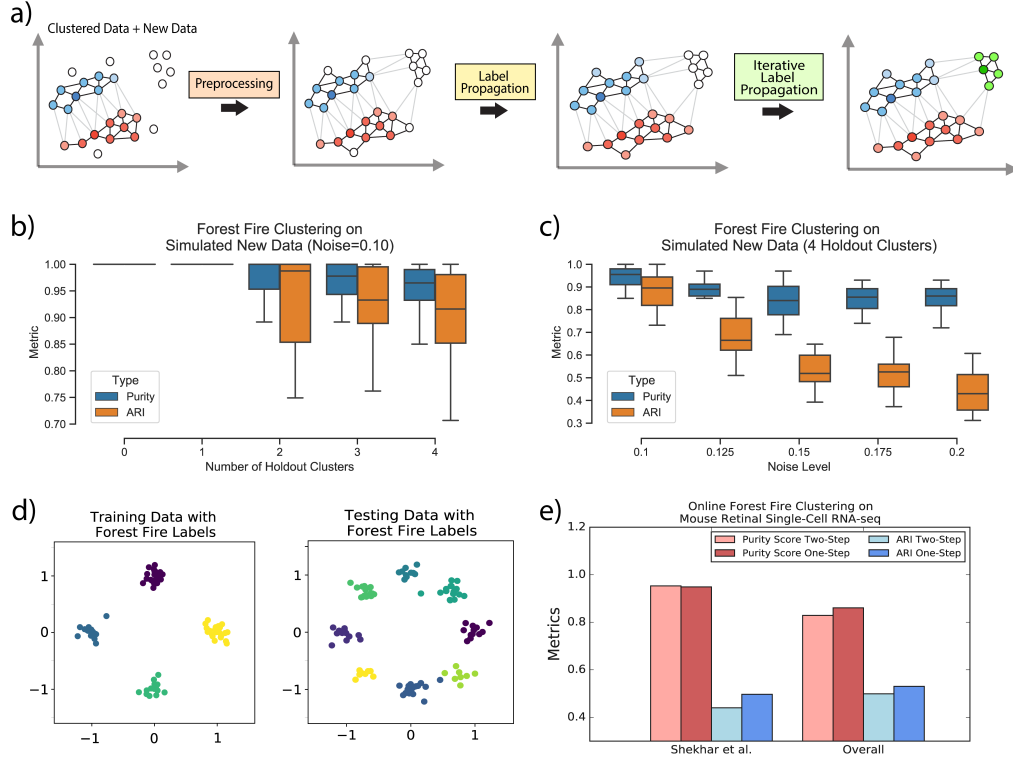


**Fig S1. Online Learning:** a) Online learning inferences can be made by extending the label from existing clusters and selecting a new seed for label propagation if new clusters arrive in the data. b) Performance of Forest Fire Clustering as the number of holdout clusters increased with  $\sigma = 0.1$ . c) Performance of Forest Fire Clustering as the noise increased with 4 holdout clusters in the testing data. d) Example of training data containing gaussian mixtures  $\sigma = 0.1$  with 4 clusters centered around the unit circle; testing data containing gaussian mixtures  $\sigma = 0.1$  with 8 clusters centered around the unit circle, 4 of which were not presented during training e) Online learning for Forest Fire Clustering on mouse retinal cell single-cell RNA-seq from *Macosko et al.* and *Shekhar et al.*. *Macosko et al.* was used as training data, and *Shekhar et al.* was used as out-of-sample data. Performance of two-step clustering remains robust compared to one-step combined clustering, showing that Forest Fire Clustering can discover new cell types in an online-learning context.

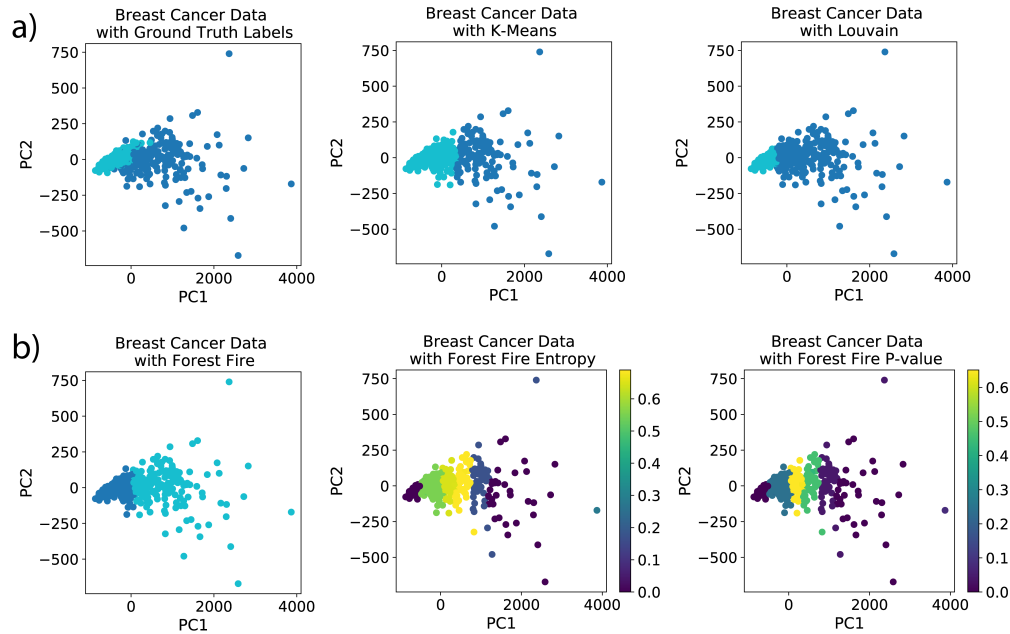


**Fig S2. Breast Cancer Malignancy Classification:** a) Breast cancer samples were categorized using K-Means, Louvain b) Breast cancer samples were categorized using Forest Fire Clustering. Internal validation was performed on Forest Fire Clustering labels. Forest Fire Clustering generated labels that best discriminate the malignancy of tumor samples compared to other clustering methods. Internal validation revealed high dimensionality and homogenous data distribution near the center.

## Acknowledgments

Research reported in this publication was supported by [name of the Institute(s), Center, or other NIH offices] of the National Institutes of Health under award number [specific NIH grant number(s) in this format: R01GM987654].

## References

1. Singh P, Singh M. Fraud Detection by Monitoring Customer Behavior and Activities. *International Journal of Computer Applications*. 2015;111(11).
2. Dunn H, Quinn L, Corbridge SJ, Eldeirawi K, Kapella M, Collins EG. Cluster Analysis in Nursing Research: An Introduction, Historical Perspective, and Future Directions. *West J Nurs Res*. 2018;40(11):1658–1676. doi:10.1177/0193945917707705.
3. Hoffman M, Steinley D, Gates KM, Prinstein MJ, Brusco MJ. Detecting Clusters/Communities in Social Networks. *Multivariate Behav Res*. 2018;53(1):57–73. doi:10.1080/00273171.2017.1391682.
4. Ding L, Feng Z, Bai Y. Clustering analysis of microRNA and mRNA expression data from TCGA using maximum edge-weighted matching algorithms. *BMC Med Genomics*. 2019;12(1):117. doi:10.1186/s12920-019-0562-z.



5. Kiselev VY, Andrews TS, Hemberg M. Challenges in unsupervised clustering of single-cell RNA-seq data. *Nat Rev Genet.* 2019;20(5):273–282. doi:10.1038/s41576-018-0088-9.
6. Saadatpour A, Lai S, Guo G, Yuan GC. Single-Cell Analysis in Cancer Genomics. *Trends Genet.* 2015;31(10):576–586. doi:10.1016/j.tig.2015.07.003.
7. Chen B, Khodadoust MS, Liu CL, Newman AM, Alizadeh AA. Profiling Tumor Infiltrating Immune Cells with CIBERSORT. *Methods Mol Biol.* 2018;1711:243–259. doi:10.1007/978-1-4939-7493-1-12.
8. DePasquale EAK, Schnell DJ, Van Camp PJ, Valiente-Alandi I, Blaxall BC, Grimes HL, et al. DoubletDecon: Deconvoluting Doublets from Single-Cell RNA-Sequencing Data. *Cell Rep.* 2019;29(6):1718–1727 e8. doi:10.1016/j.celrep.2019.09.082.
9. McGinnis CS, Murrow LM, Gartner ZJ. DoubletFinder: Doublet Detection in Single-Cell RNA Sequencing Data Using Artificial Nearest Neighbors. *Cell Syst.* 2019;8(4):329–337 e4. doi:10.1016/j.cels.2019.03.003.
10. Bernstein NJ, Fong NL, Lam I, Roy MA, Hendrickson DG, Kelley DR. Solo: Doublet Identification in Single-Cell RNA-Seq via Semi-Supervised Deep Learning. *Cell Syst.* 2020;11(1):95–101 e5. doi:10.1016/j.cels.2020.05.010.
11. Saxena A, Prasad M, Gupta A, Bharill N, Patel OP, Tiwari A, et al. A review of clustering techniques and developments. *Neurocomputing.* 2017;267:664–681.
12. Hartigan JA, Wong MA. A K-Means Clustering Algorithm. *Journal of the Royal Statistical Society.* 1979;The 28(1):8.
13. Ding C, He X. Cluster merging and splitting in hierarchical clustering algorithms. *IEEE International Conference on Data Mining.* 2002;.
14. Ester M, Kriegel H, Sander J, Xu X. A Density-Based Algorithm for Discovering Clusters in Large Spatial Databases with Noise. *Association for the Advancement of Artificial Intelligence Proceedings.* 1996;.
15. Ankerst M, Breunig MM, Kriegel HP, Sander J. OPTICS: Ordering Points To Identify the Clustering Structure. *International Conference on Management of Data.* 1999;.
16. Gan J, Tao Y. DBSCAN revisited: mis-claim, un-fixability, and approximation. In: *Proceedings of the 2015 ACM SIGMOD international conference on management of data*; 2015. p. 519–530.
17. Šubelj L. Label propagation for clustering. *Advances in Network Clustering and Blockmodeling.* 2019; p. 121–150.
18. Liang J, Zhou X, Sha Y, Liu P, Guo L, Bai S. Unsupervised Clustering Strategy Based on Label Propagation. In: *2013 IEEE 13th International Conference on Data Mining Workshops.* IEEE; 2013. p. 788–794.
19. Suzuki R, Shimodaira H. Pvcust: an R package for assessing the uncertainty in hierarchical clustering. *Bioinformatics.* 2006;22(12):1540–1542.
20. Abdelaal T, Michielsen L, Cats D, Hoogduin D, Mei H, Reinders MJ, et al. A comparison of automatic cell identification methods for single-cell RNA sequencing data. *Genome biology.* 2019;20(1):1–19.

21. Duò A, Robinson MD, Soneson C. A systematic performance evaluation of clustering methods for single-cell RNA-seq data. *F1000Research*. 2018;7.
22. Stuart T, Butler A, Hoffman P, Hafemeister C, Papalexi E, Mauck III WM, et al. Comprehensive integration of single-cell data. *Cell*. 2019;177(7):1888–1902.
23. Kiselev VY, Kirschner K, Schaub MT, Andrews T, Yiu A, Chandra T, et al. SC3: consensus clustering of single-cell RNA-seq data. *Nature methods*. 2017;14(5):483–486.
24. Zappia L, Phipson B, Oshlack A. Splatter: simulation of single-cell RNA sequencing data. *Genome biology*. 2017;18(1):1–15.
25. Shekhar K, Lapan SW, Whitney IE, Tran NM, Macosko EZ, Kowalczyk M, et al. Comprehensive Classification of Retinal Bipolar Neurons by Single-Cell Transcriptomics. *Cell*. 2016;166(5):1308–1323 e30. doi:10.1016/j.cell.2016.07.054.
26. Harris KD, Hochgerner H, Skene NG, Magno L, Katona L, Gonzales CB, et al. Classes and continua of hippocampal CA1 inhibitory neurons revealed by single-cell transcriptomics. *PLoS biology*. 2018;16(6):e2006387.
27. Macosko EZ, Basu A, Satija R, Nemesh J, Shekhar K, Goldman M, et al. Highly parallel genome-wide expression profiling of individual cells using nanoliter droplets. *Cell*. 2015;161(5):1202–1214.
28. Paul F, Arkin Y, Giladi A, Jaitin DA, Kenigsberg E, Keren-Shaul H, et al. Transcriptional heterogeneity and lineage commitment in myeloid progenitors. *Cell*. 2015;163(7):1663–1677.
29. Moon KR, van Dijk D, Wang Z, Gigante S, Burkhardt DB, Chen WS, et al. Visualizing structure and transitions in high-dimensional biological data. *Nature biotechnology*. 2019;37(12):1482–1492.
30. Wolf FA, Hamey FK, Plass M, Solana J, Dahlin JS, Göttgens B, et al. PAGA: graph abstraction reconciles clustering with trajectory inference through a topology preserving map of single cells. *Genome biology*. 2019;20(1):1–9.
31. Haghverdi L, Büttner M, Wolf FA, Büttner F, Theis FJ. Diffusion pseudotime robustly reconstructs lineage branching. *Nature methods*. 2016;13(10):845.
32. Dua D, Graff C. UCI Machine Learning Repository; 2017. Available from: <http://archive.ics.uci.edu/ml>.
33. Kiselev VY, Andrews TS, Hemberg M. Challenges in unsupervised clustering of single-cell RNA-seq data. *Nature Reviews Genetics*. 2019;20(5):273–282.
34. Aibar S, González-Blas CB, Moerman T, Imrichova H, Hulselmans G, Rambow F, et al. SCENIC: single-cell regulatory network inference and clustering. *Nature methods*. 2017;14(11):1083–1086.
35. Mika S, Schölkopf B, Smola AJ, Müller KR, Scholz M, Rätsch G. Kernel PCA and de-noising in feature spaces. In: *Advances in neural information processing systems*; 1999. p. 536–542.
36. Pedregosa F, Varoquaux G, Gramfort A, Michel V, Thirion B, Grisel O, et al. Scikit-learn: Machine Learning in Python. *Journal of Machine Learning Research*. 2011;12:2825–2830.

37. Linderman GC, Rachh M, Hoskins JG, Steinerberger S, Kluger Y. Fast interpolation-based t-SNE for improved visualization of single-cell RNA-seq data. *Nature methods*. 2019;16(3):243–245.
38. Wolf FA, Angerer P, Theis FJ. SCANPY: large-scale single-cell gene expression data analysis. *Genome biology*. 2018;19(1):1–5.